Rock magnetic and AMS fabrics characterization of suevitic breccias from the Cretaceous-Paleogene Chicxulub impact crater

**Margarita Delgadillo-Peralta, Jaime Urrutia-Fucugauchi*,
Ligia Pérez-Cruz, and Miriam Velasco-Villarreal**

*Programa Universitario de Perforaciones en Océanos y Continentes, Laboratorio de Paleomagnetismo y Paleoambientes,
Instituto de Geofísica, Universidad Nacional Autónoma de México, Coyoacán 04510 México D.F., Mexico.
juf@geofisica.unam.mx

ABSTRACT

Results of a paleomagnetic and magnetic fabrics study of the basal suevitic breccias in the Chicxulub impact crater, Yucatán platform, Gulf of Mexico are presented. The breccias were cored in the Yaxcopoil-1 borehole, which is located at about 62 km radial distance from the crater center. The impactite sequence in the Yaxcopoil-1 borehole is ~100 m thick and formed by six subunits with distinct petrographic and geochemical characteristics. Here we investigate the basal subunit interpreted as: a ground surge in the transient cavity, a melt breccia with clastic material, or an excavation flow from the ejecta curtain interacting with the ejecta plume collapse. Characterization of the magnetic fabrics using rock magnetics and anisotropy of magnetic susceptibility (AMS) are used to investigate on the emplacement mechanism of the suevites. Magnetic hysteresis and *k-T* curves show that the magnetic mineralogy is dominated by low-Ti titanomagnetites and magnetite. The AMS fabrics record mixtures of oblate and prolate ellipsoids and principal susceptibility axial distributions with relatively high angular scatter, related to turbulent high temperature conditions during ejecta emplacement. Magnetic fabric parameters and principal susceptibility axial distributions correlate with modal composition, relative contents and orientation of melt particles. Results are interpreted in terms of an emplacement mode as an early excavation flow that incorporated ground surge components.

Key words: anisotropy of magnetic susceptibility; suevite; ejecta emplacement; Yaxcopoil-1 borehole; Chicxulub crater.

RESUMEN

En este trabajo se reportan los resultados de los estudios de fábrica magnética y paleomagnéticos de las brechas suevíticas basales en el cráter Chicxulub. Las brechas han sido muestreadas en los núcleos del pozo exploratorio Yaxcopoil-1, situado a ~62 km de distancia radial del centro del cráter en el sector sur. La secuencia de impactitas en el pozo Yaxcopoil-1 tiene un espesor de ~100 m y está conformada por seis subunidades con características petrográficas y químicas distintas. En este estudio se analiza la subunidad basal de la secuencia, que ha sido interpretada en términos de: (a) un flujo tipo surge basal dentro de la cavidad transiente de excavación, (b) una brecha de roca fundida con material clástico o (c) un flujo de excavación derivado de la cortina lateral de eyecta interactuando con el colapso de la pluma central de eyecta. El mecanismo de emplazamiento de las suevitas basales se investiga a partir de análisis de propiedades magnéticas y anisotropía de susceptibilidad magnética (AMS). Los datos de histéresis magnética, magnetización remanente isotermal y curvas de susceptibilidad en función de la temperatura k-T indican que la mineralogía magnética está dominada por titanomagnetitas pobres en titanio y magnetita. La fábrica AMS se caracteriza por una mezcla de fábricas con elipsoides oblados y prolados y una distribución de los ejes principales de susceptibilidad con alta dispersión angular, relacionadas con las condiciones de alta temperatura y turbulencia generadas durante el emplazamiento. Los parámetros de fábrica magnética y la distribución angular de los ejes principales de susceptibilidad correlacionan con la composición modal y concentraciones relativas y orientaciones preferenciales de las partículas de roca fundida. Los resultados apoyan un mecanismo de emplazamiento en términos de un flujo de excavación que incorpora componentes de un flujo tipo surge basal en la etapa temprana de la cavidad de excavación.

Palabras clave: anisotropía de susceptibilidad magnética; suevitas; emplazamiento de eyecta; pozo Yaxcopoil-1; cráter Chicxulub.

INTRODUCTION

Chicxulub crater is a large ~200 km diameter multi-ring structure formed 66 Ma ago by a bolide impact in the southern Gulf of Mexico (Hildebrand *et al.*, 1991, 1998; Sharpton *et al.*, 1992; Schulte *et al.*, 2010; Urrutia-Fucugauchi *et al.*, 2011). Following formation, the crater was covered by carbonate sediments and now lies buried in the Yucatán carbonate platform. The crater preserves the ejecta deposits that have been drilled within the Chicxulub Scientific Drilling Program. The Yaxcopoil-1 borehole was drilled inside the crater in the southern sector, some 62 km away from the crater center (Urrutia-Fucugauchi *et al.*, 2004a). The impactite sequence is formed by ~100 m of melt-rich and carbonate-rich breccias with basement, melt and sedimentary clasts. High contrasts in physical properties have been documented between the carbonates, crystalline basement and melt (Urrutia-Fucugauchi *et al.*, 2004b). Petrologic, textural, mineralogical and chemical analyses

indicate that the breccias sequence is formed by distinct subunits, with varying characteristics in matrix and clast contents and composition (Stöffler *et al.*, 2004, Kring *et al.*, 2004; Tuchscherer *et al.*, 2006). The breccias subunits have been interpreted in terms of their origin, emplacement mode and post-impact alteration effects (Wittmann *et al.*, 2007).

The grain sizes, texture and composition of matrix and clasts are investigated and characterized by petrographic, geochemical and paleomagnetic studies (Urrutia-Fucugauchi *et al.*, 1996, 2004b). Logs of low-field magnetic susceptibility along the core provide information on relative distribution of carbonate and melt and basement components. Development of models proposed for emplacement of impact breccias is complicated by the high-energy and high-temperature environment, lack of observational evidence, and difficulty of scaling laboratory experiments.

In this paper, we present initial results of a rock magnetic and fabrics study of the basal carbonate-rich breccias from the sequence, recovered in the Yaxcopoil-1 borehole (Figure 1). The study forms part of the core documentation of mineralogical, chemical and physical properties and aims to characterize the magnetic properties. Further interest in analyzing the basal deposits focuses on investigating the emplacement mechanisms and crater collapse. Emplacement of the basal ejecta may involve components from the ejecta curtain and plume in the early stages, with a characteristic fabrics possibly resolvable by magnetic methods. Anisotropy of magnetic susceptibility (AMS) and rock magnetic properties have been used in studying ignimbrites and basal surge deposits and seem suited for investigating and characterizing the impact breccias.

Chicxulub Crater

The Chicxulub impact crater was first identified from the gravity and magnetic anomaly surveys conducted as part of the oil exploration programs of Petróleos Mexicanos in the Yucatán peninsula (Penfield and Camargo-Zanoguera, 1981). The Chicxulub impact has been related to the mass extinction and global environmental events marking the Cretaceous-Paleogene (K/Pg) boundary, and represents a major catastrophic event in the Phanerozoic (Hildebrand *et al.*, 1991, 1998; Schulte *et al.*, 2010). Complex multi-ring and peak-ring impact craters are formed by one of the most energetic phenomena in the geological record (Melosh, 1989). Chicxulub is one of only three large multi-ring basins documented in our planet (Collins *et al.*, 2008; Urrutia-Fucugauchi and Pérez-Cruz, 2009; Schulte *et al.*, 2010). The impact occurred in a shallow extensive carbonate platform in the southern sector of the proto-Gulf of Mexico; the crust was deformed, fragmented and pushed downwards to excavate a cavity some 25 km deep, which collapsed to form a multi-ring basin with a central uplift and inner peak-ring (Hildebrand *et al.*, 1998; Ortiz-Alemán and Urrutia-Fucugauchi, 2010; Collins *et al.*, 2008).

After formation, the basin was covered by carbonate sediments. The crater floor lies buried under about 0.8–1.0 km of carbonates, and there are no outcrops of impact lithologies in the crater region. On the surface, the buried crater rim is marked by a small semi-circular topographic depression and the cenote ring (Perry *et al.*, 1995; Connors *et al.*, 1996). As part of the recent studies in Chicxulub, drilling projects with continuous core recovery programs have been conducted (Urrutia-Fucugauchi *et al.*, 1996, 2004a, 2008, 2011). The program of the Universidad Nacional Autónoma de México (UNAM) includes
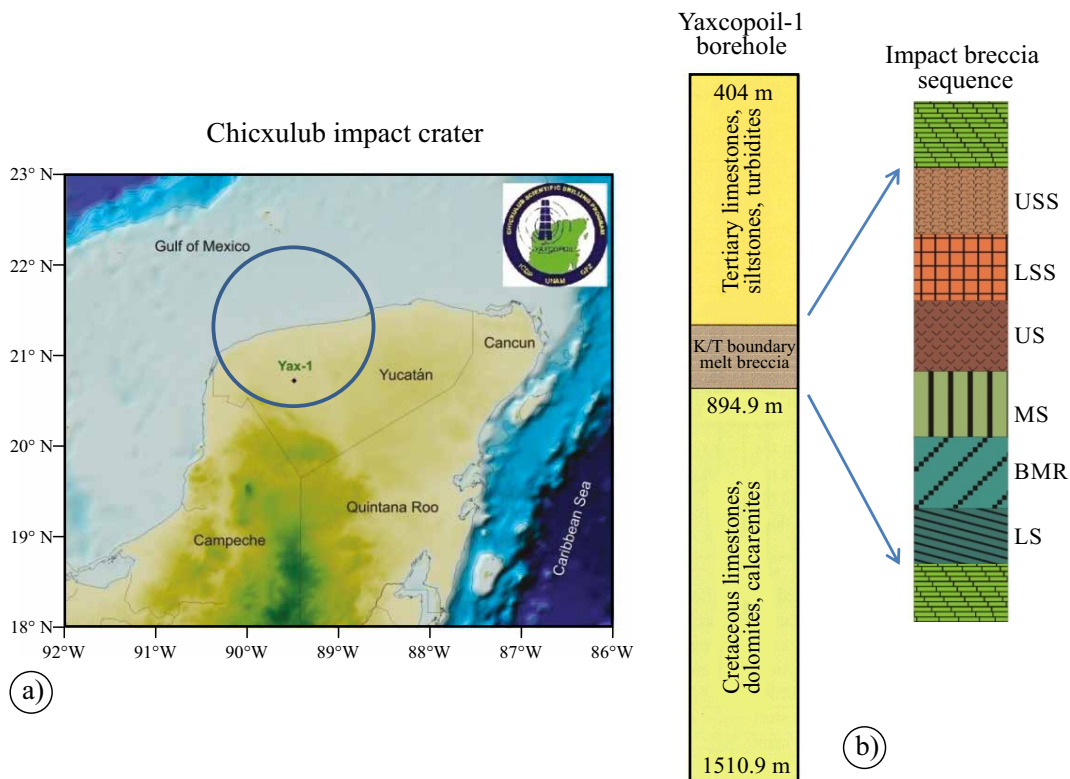

Figure 1. a) Chicxulub crater in the Yucatán platform, southern Gulf of Mexico showing location of Yaxcopoil-1 (Yax-1) borehole. b) Schematic lithological column of Yaxcopil-1 borehole with post-impact, impacties and pre-impact target sections. The impactite breccias sequence is formed by six subunits named from top to bottom as: Upper Sorted Suevite (USS), Lower Sorted Suevite (LSS), Upper Suevite (US), Middle Suevite (MS), Brecciated Impact Melt Rock (BMR) and Lower Suevite (LS).

drilling of eight boreholes in the central and southern sectors of the structure, with three boreholes (Santa Elena, Peto and Tekax) penetrating into the impact breccia sequence in the south area of the crater rim. Drilling in the inner southern sector of the crater was completed in the Chicxulub Scientific Drilling Project (CSDP) project of UNAM and the International Continental Drilling Program (Urrutia-Fucugauchi *et al.*, 2004a).

Initial rock magnetic studies in core samples from the UNAM boreholes Santa Elena, Peto and Tekax distinguished two distinct breccias sequences (Urrutia-Fucugauchi *et al.*, 1996). An upper sequence rich in basement clasts and melt fragments and a lower sequence rich in carbonate clasts, which are similar to the suevitic breccias and Bunte breccias documented in the Ries crater, Germany (Newsom *et al.*, 1986; Engelhardt *et al.*, 1995; Osinski *et al.*, 2004; Meyer *et al.*, 2011). Further, magnetic susceptibility data appeared to provide a simple proxy for the distribution and relative content of basement and melt material within the breccias. For instance, data for the upper breccia unit in UNAM-7 borehole show a trend of high susceptibility values towards the bottom of the unit, suggesting an increasing content of ferromagnetic minerals varying with depth. Susceptibility data could also be used for lateral correlation of the ejecta sequence, modeling of magnetic anomalies and study of hydrothermal activity. Hydrothermal post-impact alteration processes have affected the breccia sequence, which are reflected in the magnetic mineralogy (Urrutia-Fucugauchi *et al.*, 2004b; Pilkington *et al.*, 2004). Paleomagnetic analyses of melt and breccia samples collected from the Yucatán-1 borehole showed the occurrence of a stable remanent magnetization with an upward inclination of about 40°, which is consistent with the expected magnetic polarity at the time of the impact (Urrutia-Fucugauchi *et al.*, 1994). The K/Pg boundary occurs within the upper half of reverse polarity C29r chron, consistent with the [38]Ar/[39]Ar dates reported for melt samples from the Chicxulub-1 borehole. The age of impact and the correlation with the K/Pg boundary has been analyzed and discussed in several works (*e.g.*, Schulte *et al.*, 2010). In the boreholes drilled in the crater area, the stratigraphy of the impactites and basal carbonate sequence is being examined to constrain the sequence of events and analyze the impact effects at local and global scales.

Recent studies in the Santa Elena borehole using stable isotope and magnetic polarity stratigraphy documents the occurrence of a short hiatus following crater formation (Urrutia-Fucugauchi and Pérez-Cruz, 2008).

Magnetic susceptibility logs on the Yaxcopoil-1 cores shows a complex heterogeneous assemblage of paramagnetic, diamagnetic and ferrimagnetic minerals in the melt, basement and carbonate clasts melt and matrix (Figure 2; Urrutia-Fucugauchi *et al.*, 2004b; Pilkington *et al.*, 2004). The magnetic polarity stratigraphy documents that the normal to reverse C29r to C29n polarity transition lies within the basal carbonates in the first 50 cm interval above the breccias contact (Rebolledo-Vieyra and Urrutia-Fucugauchi, 2004). The polarity transition is consistent with the impact occurring within C29r chron.

Yaxcopoil-1 Breccia Sequence

An INDECO rotary drill equipped with a top-drive coring device were used for the drilling/coring operations. Rotary mode was employed from the surface to 404 m in depth. This interval was logged and cased. From 404 m to 1511 m, continuous wireline coring was used, which permitted to sample the complete sequence. Cores 63.5 mm diameter were obtained to a depth of 993 m, and cores 47.6 mm diameter to final depth. Yaxcopoil-1 borehole sampled the Paleogene carbonate sequence, impact breccias and overlying Cretaceous carbonates. Core recovery was 98.5 %. Cores were marked, digitally scanned and described. After completion of drilling, cores were packed and shipped to our UNAM Core Repository in Mexico City. Cores were further examined and then cut longitudinally in halves, which were again digitally scanned for high-resolution imaging (Urrutia-Fucugauchi *et al.*, 2004a, 2004b).

The breccia sequence in the Yaxcopoil-1 borehole occurs from about 794.63 m to 894.94 m in depth; the 100 m thick breccias have been divided into six subunits (Stöffler *et al.*, 2004; Kring *et al.*, 2004). From top to bottom subunits have been named as: (1) USS Upper Sorted Suevite (794-808 m), (2) LSS Lower Sorted Suevite (808-823 m), (3) US Upper Suevite (823-846 m), (4) MS Middle Suevite ((846-861 m), (5) BMR Brecciated Impact Melt Rock (861-885 m) and (6) LS Lower Suevite (885-895 m) (Figure 1).
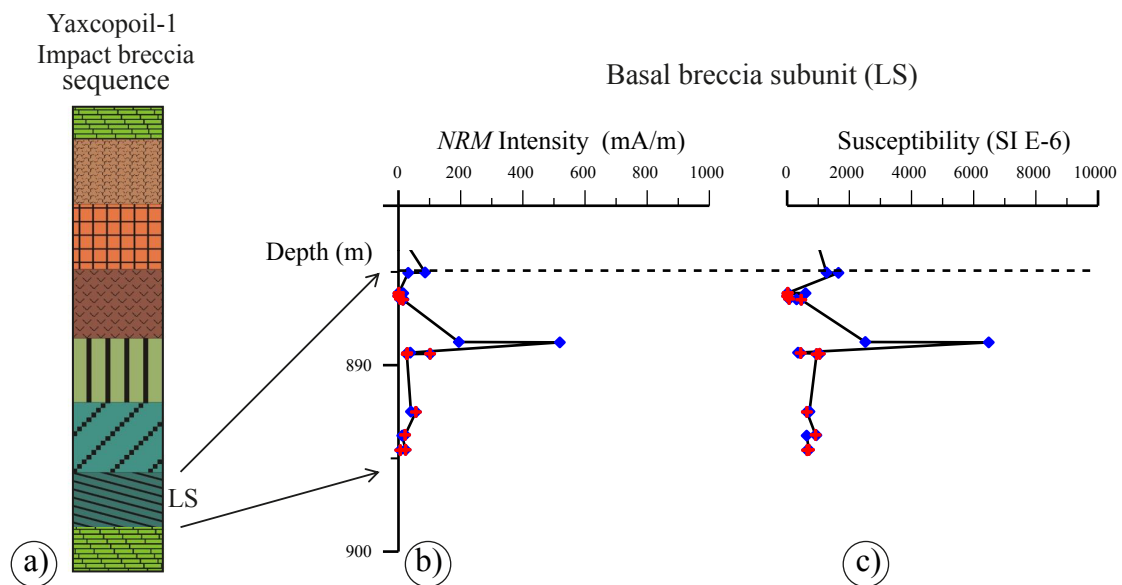

Figure 2. Natural Remanent Magnetization (*NRM*) intensity and susceptibility plotted as a function of depth for the Lower Suevite basal breccias. a) Breccia subunit division, b) *NRM* intensity c) susceptibility.

Yaxcopoil-1 Box 218 880.9–883.1 m

Yaxcopoil-1 borehole
LS subunit

Figure 3. Images of Yaxcopoil-1 borehole core segments illustrating the textures, clasts and matrix in the Lower Suevite subunit. For scale, core diameter is 63.5 mm. (a) Yax-1 core box 218, (b) Yax-1 core segment 218-9, (c) Yax-1 core segment 218-13.

The LS subunit is a variegated polymictic allogenic clast melt breccia, distinguished from the other subunits for its relative abundance, type and size of clasts, mainly composed of carbonates (Figure 3). Stöffler *et al.* (2004) described intervals formed by agglomerates of large rounded carbonates mixed with polymictic breccias with abundant melt particles, suggesting they could represent carbonate melts. The fine grained fractions are poor in lithics and rare silicate melt clasts. The LS subunit was emplaced in the early cratering stages and has been interpreted in terms of emplacement from the ejecta curtain, as a ground surge in the transient cavity, a melt breccia with clastic material and as an excavation flow with interaction with the ejecta plume (Kring *et al.*, 2004; Stöffler *et al.*, 2004; Tuchscherer *et al.*, 2006; Wittmann *et al.*, 2007).

For the paleomagnetic and AMS fabrics study, sampling was completed for the basal LS subunit of suevitic breccias, with twenty four 2.3 cm cubic samples cut between 885 m and 895 m in depth. For the magnetic hysteresis and thermomagnetic analyses, thirty additional samples were collected.

Paleomagnetic and Magnetic Fabrics

The low-field magnetic susceptibility of samples was measured using the Bartington MS2 susceptibility instrument with the dual frequency laboratory sensor. Magnetic susceptibility is in the range $0–2000 \times 10^{-6}$ SI, with higher values up to 6500×10^{-6} SI (Figure 2c). The intensity and direction of natural remanent magnetization (*NRM*) were

measured using a spinner JR6 magnetometer. *NRM* intensity shows a similar pattern to that observed in the susceptibility logs, with values in the range 0 to 100 mA/m, with a peak of about 550 mA/m (Figure 2b). The breccias are characterized by their heterogeneous nature, composed of melt particles and lithic fragments. The LS suevites contain mainly clasts of carbonate target rocks and few basement clasts. The *NRM* intensity and susceptibility logs show a peak, which corresponds to a basement clast. Low values characterize the suevite, indicating the dominance of carbonate lithics.

Magnetic mineralogy was further investigated by determining magnetic hysteresis properties and the variation of magnetic susceptibility with increasing temperature. Hysteresis loops were measured with a MicroMag system on small-sized microgram samples. Hysteresis loops and direct-field isothermal remanent magnetization (IRM) acquisition and back-field demagnetization show occurrence of low coercivity minerals (Figure 4a), possibly fine-grained magnetite and titanomagnetites.

Magnetic domain states are estimated from analysis of the ratios of hysteresis parameters (*Ms*, *Mr*, *Hc*, and *Hcr*) using the ratio plots of magnetization ratio (*Mr/Ms*) as a function of coercivity (*Hc*) (Day *et al.*, 1977; Dunlop, 2002). Hysteresis parameter ratios allow identification of domain states, with single domain (SD), pseudo-single domain (PSD) and multi-domain (MD) states. The analyzed samples are characterized by low magnetization and coercivity ratios, which plot in the PSD sector (Figure 4b).
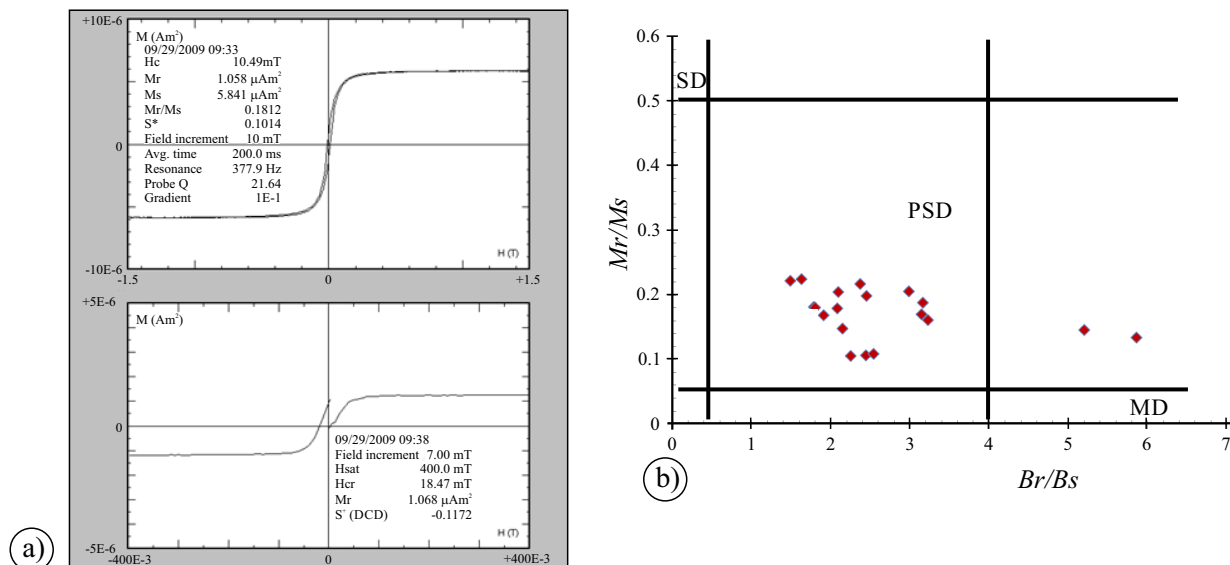
Basal breccia subunit (LS)

Figure 4. Magnetic hysteresis data. a) Examples of magnetic hysteresis loops after paramagnetic correction (top) and IRM acquisition curve and saturation IRM back-field demagnetization (bottom). b) Hysteresis parameter ratio plot showing domain state fields (SD, single domain; PSD, pseudo-single domain, and MD, multi-domain). Note that samples plot in the PSD field.

The variation of magnetic susceptibility with increasing temperature was measured with the Bartington high temperature system. Heating and cooling curves were recorded from room temperature up to 600–700 °C. The heating and cooling curves show an irreversible behavior marking relatively infrequent magnetic mineral alteration with temperature as compared to the more frequent observed case with higher susceptibilities in the cooling curves (*e.g.*, Hrouda, 2003; Hrouda *et al.*, 2003). The cooling curves fall below the heating curves, indicating dissolving titanomagnetite lamellae in less magnetic host minerals as a result of temperature alteration (Figure 5). In some of the experiments, noisy curves were measured due to the weak magnetic susceptibilities of the carbonate lithics. Curie temperatures of around 520 to 575 °C, indicative of low-Ti titanomagnetites, were determined.

AMS tensor was measured with a Kappabridge KLY-2. Data are analyzed in terms of the magnitudes and orientation of the principal susceptibility axes and the AMS parameters. Low magnitude magnetic fields applied to isotropic materials result in induced magnetizations that depend on the susceptibility of the material. In anisotropic materials, the induced magnetization is not parallel to the applied field and the angular deflection depends on the anisotropy degree. In anisotropic materials, susceptibility is represented by a second-rank tensor whose principal orthogonal axes are the maximum (K_1), intermediate (K_2) and minimum (K_3) principal susceptibilities (Tarling and Hrouda, 1993).

The relations among the magnitudes of principal susceptibilities are used to quantify the anisotropy degree ($P´$ parameter) and shape of susceptibility ellipsoid (T shape parameter) (Jelinek, 1981; Tarling and Hrouda, 1993). Magnitude and shape of susceptibility ellipsoid are determined from the shape parameter and the anisotropy degree. T-$P´$ plots permit distinction of susceptibility ellipsoid, with prolate, oblate and triaxial (neutral) ellipsoids. Oblate ellipsoids show positive T values and predominantly foliated ellipsoids. Prolate ellipsoids show negative T values and predominantly lineated ellipsoids.

The Lower Suevite is characterized by mixed prolate and oblate shaped ellipsoids. Plot of shape, T, parameter as a function of the anisotropy degree, $P´$ (Figure 6a), shows that prolate and oblate fabrics occur at low and high anisotropy degrees. In the graph, some samples show T values close to zero, which are arbitrarily marked with the discontinuous lines. This range in T parameters gives four apparent groups, which are discussed further below. The principal susceptibility axis distributions in equal-area stereographic plots show angular distributions corresponding to Fisherian, girdle and scattered distributions (Figure 6b). Prolate and oblate fabrics are distinguished with different symbols. The maximum K_1 principal axes vary from horizontal to near-vertical. In the sterograms, it can be noted that the principal axes show apparent groupings of oblate and prolate fabrics. The minimum K_3 principal axes range from shallow inclinations to vertical. Although the core was not azimuthally oriented, core segments were kept with orientation marks for the 3 m long core barrels used in the drilling/coring operations. LS subunit is characterized by mixed fabrics, with oblate and prolate shaped ellipsoids with horizontal, intermediate and near vertical axial orientations.

The AMS parameters are plotted as a function of depth, to investigate on the fabric variations along the breccia subunit (Figure 7). The mixed fabrics, with prolate and oblate shape ellipsoids are observed along the breccias interval. Marked lineated fabrics are present at three intervals, with lineated prolate ellipsoids at ~889.5 m. Foliated fabrics are observed at 889.5 m and 886 m, corresponding to high anisotropy degrees.

DISCUSSION

The impactite sequence cored in the Yaxcopoil-1 borehole (Figure 1) is formed by six distinct subunits, which are characterized by distinct composition, texture, matrix type and relative contents and type of basement, melt and carbonate particles. Clasts show different morphologies, sizes, preferential alignments and alteration degrees. Rock magnetic analyses take advantage of the high contrasts between the sedimentary clasts, carbonate-rich matrix, melt and basement clasts and melt-rich matrix. The variations in magnetic mineralogy, grain sizes
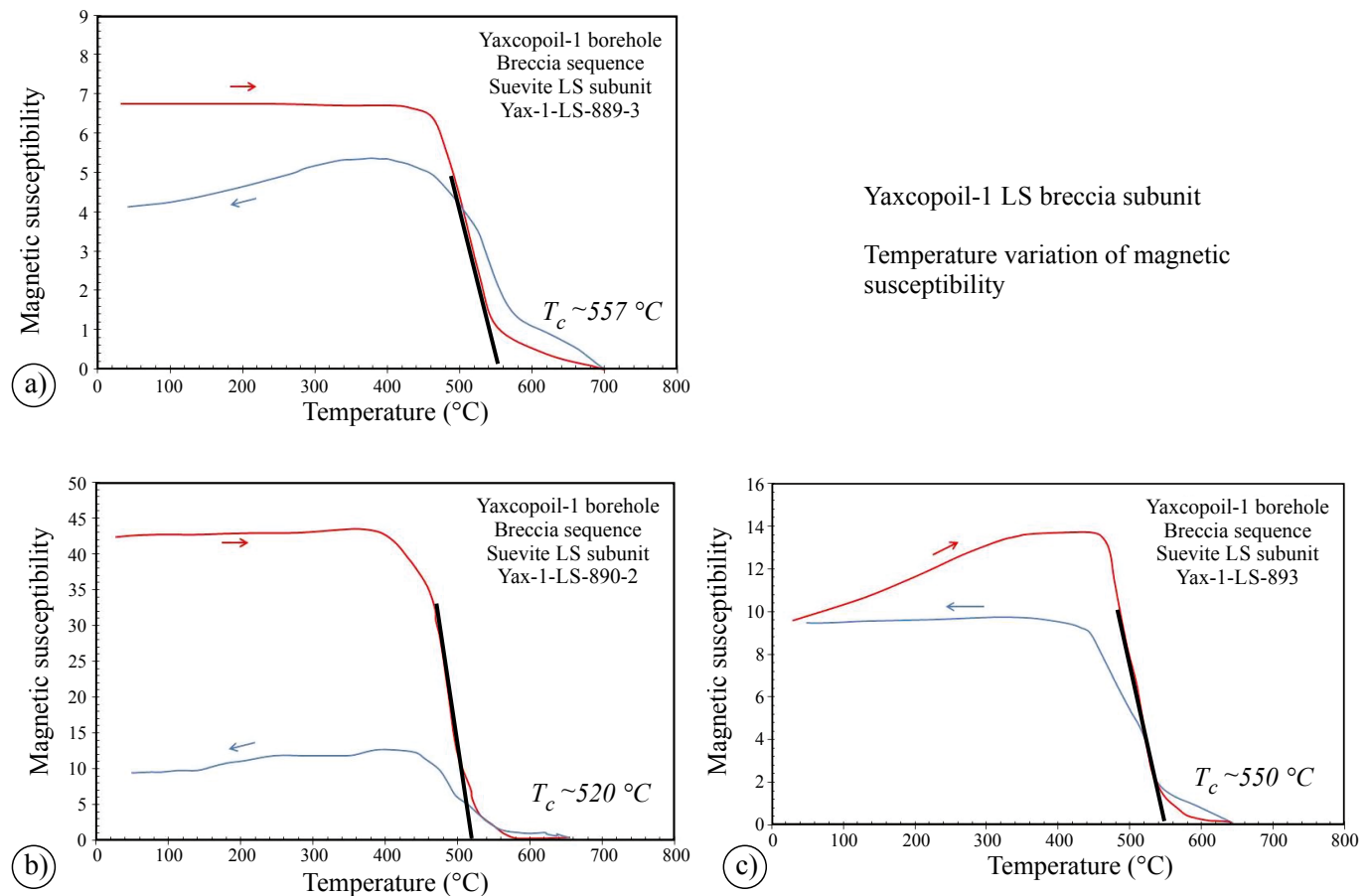
Figure 5. Temperature variation of magnetic susceptibility. Characteristic examples of heating/cooling curves of low-field magnetic susceptibility as a function of increasing temperature for samples of the LS suevites.

and textures along the Yaxcopoil-1 subunits are recorded in the magnetic susceptibility logs (Urrutia-Fucugauchi *et al.*, 2004b; Pilkington *et al.*, 2004). The basal subunit formed in the early stages of cratering has been interpreted as: a) a ground surge in the transient cavity, b) a melt breccia with clastic material, and c) an excavation flow from the ejecta curtain interacting with the ejecta plume collapse (Stöffler *et al.*, 2004; Kring *et al.*, 2004; Tuchscherer *et al.*, 2006).

Magnetic susceptibility and *NRM* intensities are low in the LS subunit (Figure 8), corresponding to its carbonate-rich character. The low-frequency susceptibility ranges from 5.48–6485 × 10⁻⁶ SI, with a mean value of 889.51 × 10⁻⁶ SI. The *NRM* intensity varies from 0.07 to 519.1 mA/m, around mean values of 52 mA/m. *NRM* intensity and susceptibility distributions are skewed to low values (Figure 8a, 8b), characterized by log-normal distributions. The anisotropy degree varies from low to high anisotropies with a range of *P′* values from 1.01 up to 1.12 (Figure 8c). Samples with oblate shaped ellipsoids tend to present low *NRM* intensities and susceptibilities and those with lineated fabrics show high *NRM* intensities and susceptibilities (Figure 8e). The *NRM* intensities and susceptibilities correlate, particularly for the prolate fabrics. Relationships with anisotropy degree appear more complex. Oblate fabrics show weak susceptibilities and a wide range of *P′* values, from weak anisotropies to strong anisotropies (Figure 8d). Prolate fabrics show narrow range in anisotropy degree (except for an anomalous value of 1.09) and a rough tendency to decrease with increasing susceptibility. This is better displayed in a semi-log graph; the anisotropy degree shows a tendency to decrease with increasing

bulk susceptibility, and the tendency is apparent for both the oblate and prolate fabrics (Figure 8f).

Distribution of the principal susceptibility axes gives the axial orientations for prolate shaped and oblate ellipsoids (Figure 6b). Prolate ellipsoids show K_1 lineation, with intermediate to shallow dips. Oblate ellipsoids show K_1 axes with intermediate to steep dips. Wittmann *et al.* (2007) discussed the emplacement mechanisms for the impactite sequence in Yaxcopoil-1 borehole from petrologic and image analytical analyses of core samples. They proposed that emplacement of the LS began in the first minute after impact, with the ejecta curtain interacting with the high volume ejecta plume. Their reconstruction relied on the petrographic characteristics and modal compositional variations, using relative abundance, size distributions, preferred alignment and shape parameters (elongation) of melt particles. Melt particles have been described and characterized by detailed petrographic and geochemical analyses in several studies (Kring *et al.*, 2004; Stöffler *et al.*, 2004; Tuchscherer *et al.*, 2006). Melt particles are highly magnetic compared to the carbonate-rich matrix and carbonate clasts. Therefore, possible correlation with the AMS derived fabrics could be expected.

The modal compositions, with relative contents of melt particles, basement and sedimentary clasts and matrix for the LS subunit are summarized in Figure 9a as a function of depth (Wittmann *et al.*, 2007). Melt particles are characterized by high magnetic susceptibilities and *NRM* intensities (Urrutia-Fucugauchi *et al.*, 2004b; Pilkington *et al.*, 2004). Melt particles present in the LS are type 3 brecciated melt rock particles and type 3 schlieren melt particles. Melt particles types 4 and
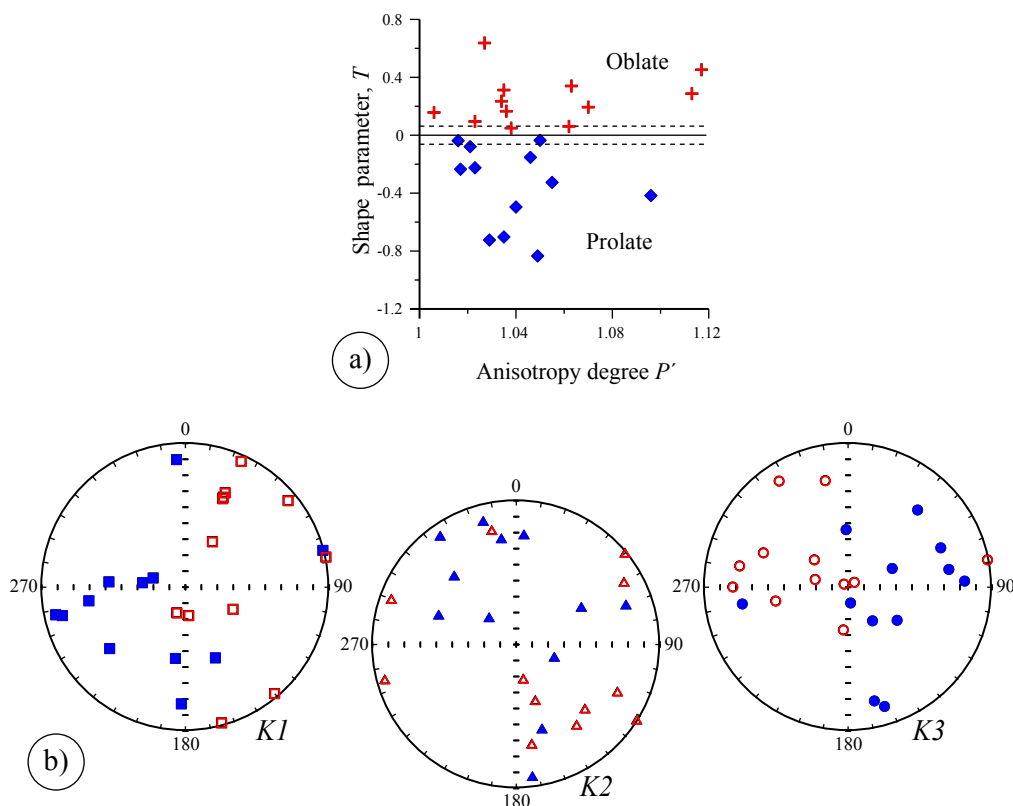
Figure 6. AMS fabric parameters and principal susceptibility axial distributions. a) Plot of shape parameter *T* as a function of anisotropy degree *P´*, showing occurrence of prolate and oblate spheroids. b) Principal susceptibility axial distributions plotted in equal-area nets for the K_1, K_2 and K_3 axis. The blue symbols correspond to prolate spheroids and the red symbols to oblate spheroids.

1 are rare and there are no type 2 melt particles. Matrix represents about 40 % in volume up to 60 %. Basement clasts are less abundant and sedimentary carbonate clasts are around 20 %, reaching up to 70 % in the upper half of the subunit. The component size distribution covers the range 0.5 to 64 mm with mode of 4-2 mm; data are shown in a histogram in Figure 9b.

The depth patterns of modal composition data (Figure 9a) show a rough correlation with the AMS parameter data (Figure 7), with the peaks of lineation, foliation and anisotropy degree corresponding to the increases in type 3 BMR and schlieren melt particles. Lack of type 2 and low contents of type 4 melt particles in the LS indicate absence of airborne deposition for the subunit (Stöffler *et al.*, 2004; Wittmann *et al.*, 2007). The long axes of elongated melt particles show a tendency to lie in the horizontal plane (Figure 9c), with shallow dips determined from their relative orientation with respect to the core up-down axis. Dips vary from steep to shallow, which is also apparently observed for the prolate ellipsoids K_3 axes. Similar patterns are observed for the oblate ellipsoids. Possible controls on the AMS fabrics with relative contents and distribution of type 3 BMR and schlieren melt particles require further analysis. The modal compositional data and the trend of elongation of melt particles and high scatter pattern seems consistent with the excavation-flow model of Shuvalov (2003) of ejecta flows interacting with the ejecta plume. The LS subunit represents a mixture of material from the shallow carbonate target sequence and deeply excavated basement rocks (stream-tube depositional model of Stöffler *et al.*, 2004).

AMS studies are used in understanding emplacement mechanisms and conditions of ignimbrites, lavas, intrusive bodies and sediments.

Studies documented the spatial relationships between the principal susceptibility axes and the emplacement and flow mode and directions (*e.g.*, Paquereau-Lebti *et al.*, 2008; Petronis and Geissman, 2009; LaBerge *et al.*, 2009). On the other hand, there are relatively few studies of emplacement mode and fabric characteristics of impact breccias, which may present characteristics similar to those recorded in ignimbrites and ground surges. This might be particularly the case for suevitic units emplaced as part of the ejecta curtain and basal surges. This emplacement mode has been suggested for the basal suevitic LS subunit by Stöffler *et al.* (2004), which may have involved dynamic conditions of high turbulence and hot gases at the floor of the transient cavity. High temperature turbulent conditions are suggested by the characteristics of melt particles and lithics in the LS. Carbonate clasts are metamorphosed with incipient resorption. Zircons show coarse recrystallization during prolonged annealing at temperatures above 700 ºC. Melt particles are unsorted and shape oriented consistent with formation in a low viscosity melt rapidly quenched (Wittmann *et al.*, 2007).

For interpretation of the magnetic fabric of the impact breccias, reference to observations on high energy sedimentary and pyroclastic flows provides an analogy (*e.g.*, Tarling and Hrouda, 1993; Capaccioni *et al.*, 2001; Petronis and Geissman, 2009). In particular, correlation with AMS fabrics in ignimbrites and ground surges provide additional insight on the nature of magnetic fabrics in suevites (Rochette and Filion, 1988; Rochette *et al.*, 1992; Paquereau-Lebti *et al.*, 2008; Petronis and Geissman, 2009). AMS studies on debris gravity flows, turbidites, ignimbrites and ground surges have shown flow parallel and flow transverse dominant orientations. Hot turbulent basal surges and laminar
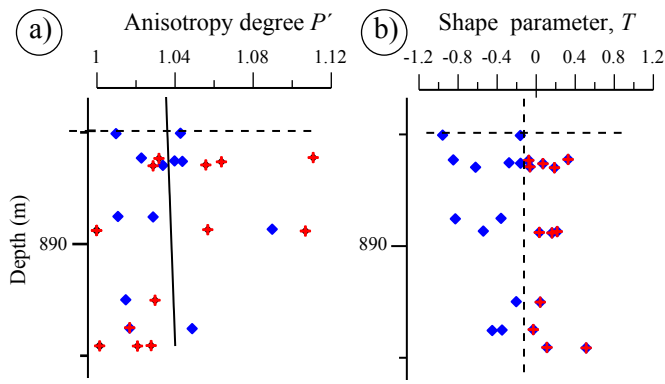
Figure 7. Magnetic fabric parameters plotted as a function of depth. a) Anisotropy degree *P´*, and b) Shape parameter *T*.

flows have distinctive magnetic fabrics, where maximum axes tend to lie parallel to flow directions with minimum axes normal to foliation planes (Cagnoli and Tarling, 1997). In some cases, maximum axes are the ones oriented perpendicular to flow directions (MacDonald and Palmer, 1990; Tarling and Hrouda, 1993; Cagnoli and Tarling, 1997).

Within-flow alignment variations, scattered and girdle axial distributions of grains in ignimbritic flows have been observed and related to emplacement conditions and flow characteristics (*e.g.*, MacDonald and Palmer, 1990; Ort *et al.*, 2003; LeBerge *et al.*, 2009). LeBerge *et al.* (2009) recorded small and large scale variations in AMS determined

flow directions trough vertical sections of ignimbrites. They discussed possible mechanisms for grain orientation alignment and scattered axial distributions, in terms of meandering and shear effects modifying the particle concentration capacity of flows. One of the mechanisms involves microtopography and eddy effects of coarse grains disrupting coherent fine grain alignment. Increase of grain orientation scatter will result from higher deposition rates, occurring for instance from particles settling from the top of the flow. Another mechanism involves shearing with formation of a sheared bed controlled by substrate rigidity and cohesiveness. Meandering flows with varying particle concentration and velocity above the sheared zone will result in different grain orientations.

The LS subunit show abundant carbonate lithics possibly incorporated from the target substrate. The lithics display a wide range of thermal effects from melted clasts to unmetamorphosed clasts with microfossils preserved (Tuchscherer *et al.*, 2006). Melt particles tend to be elongated and randomly oriented and there are no fallout airborne transported particles. The suevites contain a range of melt particles and lithics of varying sizes, which may result in meandering, shearing and chaotic alignment of the fine particles, resulting in scattered axial distributions as observed for the basal pyroclastic surges (LeBerge *et al.*, 2009). The long axes of melt particles tend to lie in the horizontal plane (Figure 9c). These characteristics appear consistent with a surge emplacement mechanism of an excavation flow interacting with the ground and the collapsing ejecta plume (Wittmann *et al.*, 2007).

Part of the apparent scatter in the principal axis distribution observed for the prolate and oblate fabrics could arise from inverse fabrics, affecting the K_1 and K_3 axes. For the oblate fabrics, angular scatter is
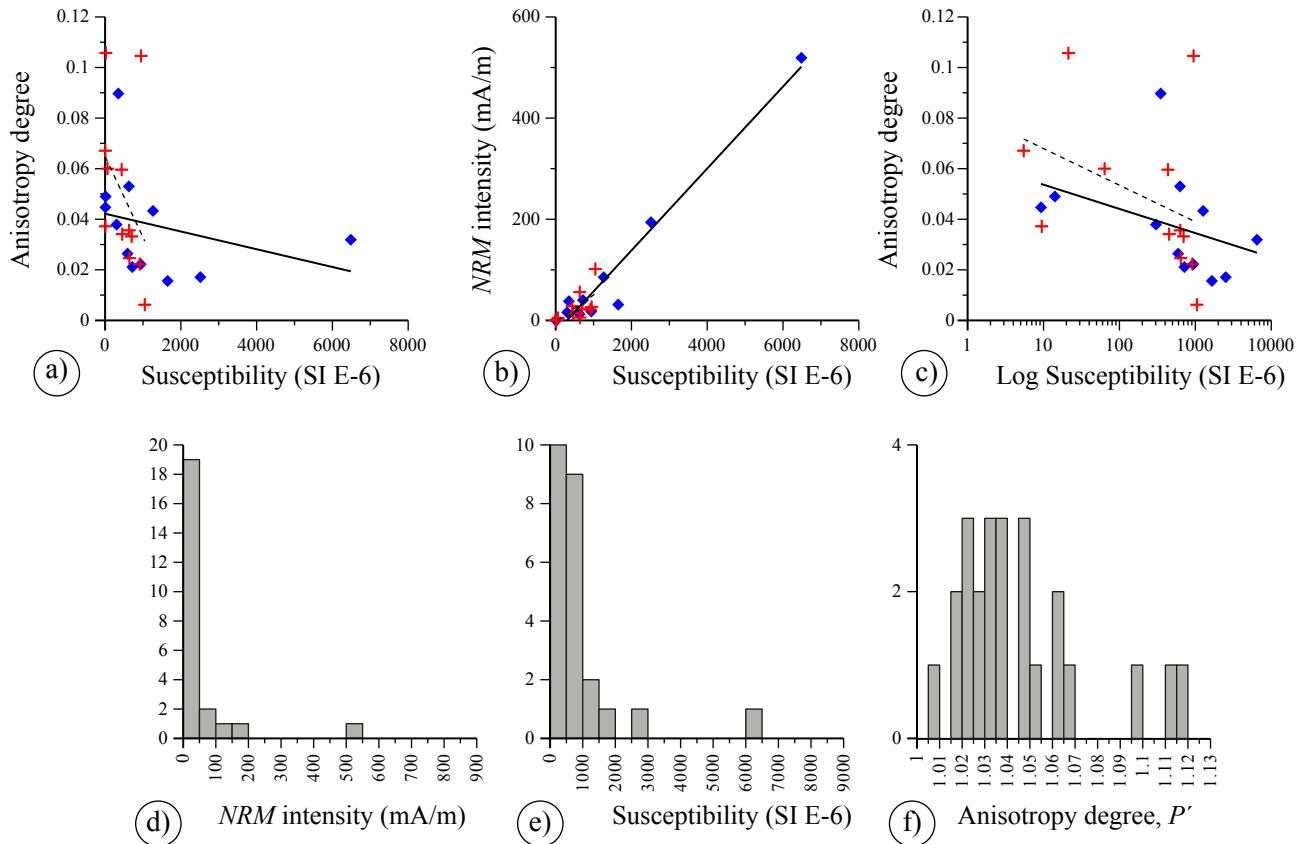

Figure 8. Plots of a) anisotropy degree versus susceptibility, b) *NRM* intensity versus susceptibility and c) anisotropy degree versus log susceptibility. Histograms of d) *NRM* intensity, e) susceptibility and f) anisotropy degree.
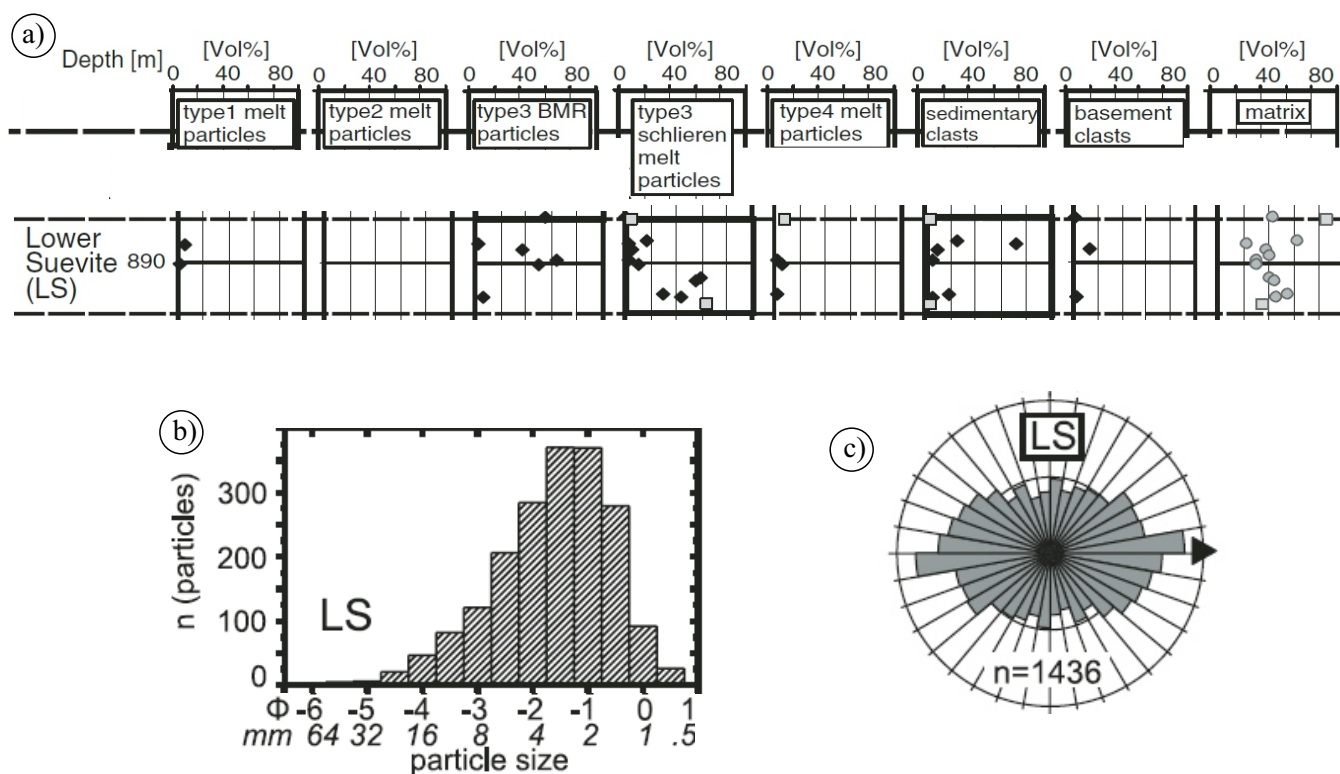
Figure 9. Melt particles in the LS suevites (taken from Wittmann *et al.* (2007). a) Modal compositions, with relative contents of melt particles, basement and sedimentary clasts and matrix for the LS subunit plotted as a function of depth. b) Histogram of melt particle size. The component size distribution covers the range 0.5 to 64 mm with a mode of 4-2 mm. c) Rose diagram for the dips of long-axis orientation of melt particles referred to the drill core axis. Note that the long axes of elongated melt particles show a tendency to lie in the horizontal plane, with shallow dips determined from their relative orientation with respect to the core up-down axis. Dips vary from steep to shallow.

reduced for instance if shallow minimum K_3 axes and near vertical maximum K_1 axes are inverted. Inverse fabrics have been observed in volcanic and sedimentary rocks, where their maximum axes lie perpendicular to apparent dominant flow directions (Rochette *et al.*, 1992; Ferré, 2002; Tarling and Hrouda, 1993). Multi-domain magnetite assemblages have maximum axes parallel to particle long axes. For assemblages of single-domain magnetites, maximum axes tend to be perpendicular to particle long axes (Potter and Stephenson, 1988). The hysteresis ratio plots show predominant PSD domain states for the LS subunit (Figure 4), which may represent a mixture of SD and MD particles. Detailed study of magnetic domain states are required to assess dependency of AMS axial distribution on dominant domain state. For heterogeneous breccias, separation of paramagnetic and diamagnetic contributions may become important. Intermediate fabrics not simply related to any given magnetic grain anisotropy may arise, which may be the case for the LS subunit in the impact breccias sequence.

The magnetic hysteresis and temperature variation of magnetic susceptibility show magnetic minerals with Curie temperatures ranging from 520 to 575 °C and hysteresis loops with high saturation magnetizations, indicating that the main magnetic minerals are low-Ti titanomagnetites. The hysteresis parameter ratio plot shows that most samples plot in the PSD domain field. The heating/cooling curves of magnetic susceptibility with increasing temperature show irreversible behavior. The cooling curves fall below the heating curves suggesting dissolving titanomagnetite lamellae in less magnetic host minerals, which is relatively infrequent as compared to production of magnetite during heating to temperatures of 600–700 °C. The alteration of magnetic mineralogy during laboratory heating has been investigated in

several studies, providing evidence for temperature-induced alterations (Hrouda, 2003; Hrouda *et al.*, 2003). Another factor to consider in the rock magnetic analysis is the effects of hydrothermal alteration. In large impacts, the high temperatures result in formation of a coherent melt sheet and generation of a long-lived hydrothermal system. Effects of hydrothermal alteration result in formation of secondary minerals, affecting the remanent magnetization and opaque minerals (Ade-Hall *et al.*, 1971; Sweetkind *et al.*, 2012). Rock magnetic analyses in the Chicxulub breccias have been documented, with formation of Fe–Ti oxide minerals (Pilkington *et al.*, 2004; Kring *et al.*, 2004; Urrutia-Fucugauchi *et al.*, 2004b). The effects of hydrothermal alteration on the AMS and magnetic susceptibility in the LS subunit require further investigation.

The effects of shock on the magnetic properties and magnetization record have been long studied (*e.g.*, Cisowski and Fuller, 1978; Halls, 1979). Shock induced effects on the AMS have been analyzed experimentally, to further understand the effects on target materials. Correlation of magnetic properties on target rocks with the direction of impact has also been examined for the Lonar crater (Arif *et al.*, 2012). Rock magnetic properties in the target basalts are symmetrically oriented with respect to the plane of impact. Laboratory experiments have shown that impacts change the remanent magnetization, resulting in demagnetization and remagnetization effects, with changes in the coercivity (Gattacceca *et al.*, 2007). The AMS axial distribution has also been shown to be affected, with principal susceptibility directions reoriented to the shock axis (Gataccceca *et al.*, 2007; Nishioka *et al.*, 2007). Nishioka *et al.* (2007) analyzed the shock effects on basalt target samples with pressures up to 5 GPa, showing that the maximum

and minimum axes are reoriented with changes in the AMS ellipsoidal shape and anisotropy degree. Changes in ellipsoid shape were more pronounced for samples close to the impact point, with no appreciable changes for samples farther from impact point. Variation of shock pressure in target and impact-generated lithologies can then result in varying degrees of fabrics modification.

CONCLUSIONS

The AMS fabrics are characterized by oblate and prolate ellipsoids with principal susceptibility axial distributions showing high angular scatter, related to turbulent high temperature conditions during emplacement. Breccias with oblate ellipsoids tend to present low *NRM* intensities and susceptibilities and those with developed lineated fabrics show high *NRM* intensities and susceptibilities. The *NRM* intensities and susceptibilities show similar patterns, particularly for the prolate fabrics. Oblate fabrics show weak susceptibilities and wide range of P' values, from weak anisotropies to strong anisotropies. Prolate fabrics show narrow ranges in anisotropy degree with a tendency to decrease with increasing susceptibility. Anisotropy degree tends to decrease with increasing bulk susceptibility for oblate and prolate fabrics.

The oblate fabrics show K_1 axes with intermediate to steep dips. Prolate ellipsoids show K_1 lineation, with intermediate to shallow dips. Long axes of elongated melt particles tend to lie in the horizontal plane. Long axis particle dips, however, vary from steep to shallow, which is also observed for prolate and oblate ellipsoid K_1 and K_3 axes. Considering that the LS subunit shows mixture of material from shallow carbonate target and deep basement rocks (Kring *et al.*, 2004; Stöffler *et al.*, 2004; Wittmann *et al.*, 2007), suevites were likely emplaced as an excavation flow incorporating ground surge material. Studies in the Ries crater have shown that elongated particles in the suevites are distributed radially or concentrically, consistent with a lateral transport mechanism (Meyer *et al.*, 2011). This emplacement mechanism involves horizontal transport under high temperature turbulent conditions, similar to basal surges, plus ejecta plume collapse components. Modeling of suevite emplacement mechanisms however remains difficult because of the turbulent high energy high temperature environment.

ACKNOWLEDGMENTS

REFERENCES

Ade-Hall, J.M., Palmer, H.C., Hubbard, T.P., 1971, The magnetic and opaque petrological response of basalts to regional hydrothermal alteration: Geophysical Journal Royal Astronomical Society, 24, 137-174.

Arif, M., Basavaiah, N., Misra, S., Deenadayalan, K., 2012, Variations in magnetic properties of target basalts with the direction of asteroid impact: Example from Lonar crater, India: Meteoritics and Planetary Science, 47(8), 1305-1323.

Capaccioni, B., Nappi, G., Valentini, L., 2001, Directional fabric measurements: An investigative approach to transport and depositional mechanisms in pyroclastic flows: Journal Volcanology and Geothermal Research, 107(4), 275-292.

Cagnoli, B., Tarling, D.H., 1997, The reliability of anisotropy of magnetic susceptibility (AMS) data as flow indicators in friable base surge and ignimbrite deposits: Italian examples: Journal Volcanology and Geothermal Research, 75(3), 309-320.

Cisowski, S.M., Fuller, M., 1978, The effect of shock on the magnetism of terrestrial rocks: Journal of Geophysical research, 83(B7), 3441-3458.

Collins, G.S., Morgan, J., Barton, P., Christeson, G.L., Gulick, S., Urrutia-Fucugauchi, J., Warner, M., Wünnemann, K., 2008, Dynamic modeling suggests terrace zone asymmetry in the Chicxulub crater is caused by target heterogeneity: Earth Planetary Science Letters, 270(3), 221-230. doi: 10.1016/j.epsl.2008.03.032

Connors, M., Hildebrand, A.R., Pilkington, M., Ortiz-Aleman, C., Chavez, R.E., Urrutia-Fucugauchi, J., Graniel-Castro, E., Camara-Zi, A., Vasquez, J., Halpenny, J.F., 1996, Yucatán karst features and the size of Chicxulub crater: Geophysical Journal International, 127(3), F11-F14.

Day, R., Fuller, M.D., Schmidt, V.A., 1977, Hysteresis properties of titanomagnetites: grain size and composition dependence: Physics of the Earth and Planetary Interiors, 13(4), 260-266.

Dunlop, D.J., 2002, Theory and application of the Day plot (M_{rs}/M_s versus $H_{cr}/H_c)_1$. Theoretical curves and tests using titanomagnetite data: Journal of Geophysical Research, 107 (B3), doi: 10.1029/2001JB000486.

Engelhardt, W. V., Arndt, J., Fecker, B., Pankau, H. G., 1995, Suevite breccia from the Ries crater, Germany: Origin, cooling history and devitrification of impact glasses: Meteoritics and Planetary Science, 30(3), 279-293.

Ferré, E.C., 2002, Theoretical models of intermediate and inverse AMS fabrics: Geophysical Research Letters, 29(7), 31-1–31-4.

Gattacceca, J., Lamali, A., Rochette, P., Boustie, M., Berthe, L., 2007. The effects of explosive-driven shocks on the natural remanent magnetization and the magnetic properties of rocks: Physics of the Earth and Planetary Interiors, 162, 85-98.

Halls, H.C., 1979, The Slate Islands meteorite impact site: a study of Shock Remanent Magnetization: Geophysical Journal of the Royal Astronomical Society, 59(3), 553-591.

Hildebrand, A.R., Penfield, G.T., Kring, D.A., Pilkington, M., Camargo, A., Jacobsen, S.B., Boynton, W.V., 1991, Chicxulub Crater: a possible Cretaceous/Tertiary boundary impact crater on the Yucatán Peninsula, Mexico: Geology, 19(9), 867-871.

Hildebrand, A.R., Pilkington M., Ortíz-Aleman, C., Chávez R.E., Urrutia-Fucugauchi, J., Connors M., Graniel-Castro E., Camara-Zi, A., Halpenny, J.F., Niehaus D., 1998, Mapping Chicxulub crater structure with gravity and seismic reflection data: Geological Society, London, Special Publications, 140, 155-176.

Hrouda, F., 2003, Indices for numerical characterization of the alteration processes of magnetic minerals taking place during investigation of temperature variation of magnetic susceptibility: Studia Geophysica et Geodaetica, 47(4), 847-861.

Hrouda, F., Müller,, P., Hanák, J., 2003, Repeated progressive heating in susceptibility vs. temperature investigation: a new palaeotemperature indicator?: Physics and Chemistry of the Earth, 28(16-19), 653-657.

Jelinek, V., 1981, Characterization of the magnetic fabric of rocks: Tectonophysics, 79(3-4), T63-T67.

Kring, D.A., Hörz, F., Zurcher, L., Urrutia-Fucugauchi, J., 2004, Impact lithologies and their emplacement in the Chicxulub impact crater: Initial results from the Chicxulub scientific drilling project, Yaxcopoil, Mexico: Meteoritics and Planetary Science, 39(6), 879-897.

LaBerge, R.D., Porreca, M., Mattei, M., Giordano, G., Cas, R.A.F., 2009, Meandering flow of a pyroclastic density current documented by the anisotropy of magnetic susceptibility (AMS) in the quartz latite ignimbrite of the Pleistocene Monte Cimino volcanic center (central Italy): Tectonophysics, 466(1), 64-78.

MacDonald, W.D., Palmer, H.C., 1990, Flow directions in ash-flow tuffs: a comparison of geological and magnetic susceptibility measurements, Tshirege member (upper Bandelier Tuff), Valles caldera, New Mexico, USA: Bulletin Volcanology, 53(1), 45-59.

Melosh, H. J., 1989, Impact cratering: A geologic process. Research supported by NASA: New York, Oxford University Press (Oxford Monographs on Geology and Geophysics, No. 11), 1, 253 pp.

Meyer, C., Jébrak, M., Stöffler, D., Riller, U., 2011, Lateral transport of suevite

inferred from 3D shape-fabric analysis: Evidence from the Ries impact crater, Germany: Geological Society of America Bulletin, 123(11-12), 2312-2319.

Newsom, H.E., Graup, G., Sewards, T., Keil, K., 1986, Fluidization and hydrothermal alteration of the suevite deposit at the Ries crater, West Germany, and implications for Mars: Journal of Geophysical research: Solid Earth, 91(B13), E239-E251.

Nishioka, I., Funaki, M., Sekine, T., 2007, Shock-induced anisotropy of magnetic susceptibility: impact experiment on basaltic andesite: Earth, Planets and Space, 59, e45-e48.

Osinski, G.R., Grieve, R.A.F., Spray, J.G., 2004, The nature of the groundmass of surficial suevite from the Ries impact structure, Germany, and constrains on its origin: Meteoritics and Planetary Science, 39(10), 1655-1683.

Ort, M.H., Orsi, G., Pappalardo, L., Fisher, R.V., 2003, Anisotropy of magnetic susceptibility studies of depositional processes in the Campanian Ignimbrite, Italy: Bulletin of Volcanology, 65(1), 55-72.

Ortiz-Alemán, C., Urrutia-Fucugauchi, J., 2010, Aeromagnetic anomaly modeling of central zone structure and magnetic sources in the Chicxulub crater: Physics of the Earth and Planetary Interiors, 179, 127-138.

Paquereau-Lebti, P., Fornari, M., Roperch, P., Thouret, J.C., Macedo, O., 2008, Paleomagnetism, magnetic fabric, and 40Ar/39Ar dating of Pliocene and Quaternary ignimbrites in the Arequipa area, southern Peru: Bulletin of Volcanology, 70(8), 977-997.

Penfield, G.T., Camargo-Zanoguera, A. 1981, Definition of a major igneous zone in the central Yucatán platform with aeromagnetics and gravity, *in* Society of Exploration Geophysicists, 51st Annual Meeting: Tulsa, Oklahoma, Society of Exploration Geophysicists, Technical Program, Abstracts and Bibliographies, 37.

Perry, E.C., L. Marin, J. McClain, G. Velazquez, 1995, The ring of cenotes (sinkholes), Northwest Yucatán, Mexico: Its hydrogeologic characteristics and possible association with the Chicxulub impact crater: Geology, 23(1), 17–20.

Petronis, M.S., Geissman, J.W., 2009, Anisotropy of magnetic susceptibility data bearing on the transport direction of mid-Tertiary regional ignimbrites, Candelaria Hills area, West-Central Nevada: Bulletin Volcanology, 71(2), 121-151.

Pilkington, M., Ames, D., Hildebrand, A.R., 2004, Magnetic mineralogy of the Yaxcopoil-1 core, Chicxulub crater: Meteoritics Planetary and Science, 39(6), 831-842.

Potter, D.K., Stephenson, A., 1988. Single-domain particles in rocks and magnetic fabric analysis: Geophysical Research Letters, 15(10), 1097-1100.

Rebolledo-Vieyra, M., Urrutia-Fucugauchi, J., 2004, Magnetostratigraphy of the impact breccias and post-impact carbonates from borehole Yaxcopoil-1, Chicxulub impact crater, Yucatán, Mexico: Meteoritics and Planetary Science, 39(6), 821-830.

Rochette, P., Fillion, C., 1988, Identification of multicomponent anisotropies in rocks using various field and temperature values in a cryogenic magnetometer: Physics of the Earth and Planetary Interiors, 51(4), 379-386.

Rochette, P., Jackson, M., Aubourg, C., 1992, Rock magnetism and interpretation of anisotropy of magnetic susceptibility: Reviews of Geophysics, 30(3), 209-226.

Schulte, P., Alegret L., Arenilla, I., Arz, J.A., Barton, P.J., Bown, P.R., Bralower, T., Christeson, G.L., Claeys, P., Cockell,, C.S., Collins, G.S., Deutsch, A., Goldin, T., Goto, K., Grajales, J.M., Grieve, R.A.F., Gulick, S., Johnson, K., Kiessling, W., Koeberl, C., Kring, D.A., MacLeod, K.G., Matsui, T., Melosh, J., Montanari, A., Morgan, J., Neal, C.R., Nichols D., Norris R.D., Pierazzo E., Ravizza R., Rebolledo, M., Reimold, W.U., Robin, R., Salge, T., Speijer, R.P., Sweet, A., Urrutia-Fucugauchi, J., Vajda, V., Whalen, M.T., Willumsen, P.S., 2010, The Chicxulub asteroid impact and mass extinction at the Cretaceous-Paleogene boundary: Science, 327, 1214-1218.

Sharpton, V.L., Dalrymple, G., Marin, L., Ryder, G., Schuraytz, B., Urrutia-Fucugauchi, J., 1992, New links between the Chicxulub impact structure and the Cretaceous/Tertiary boundary: Nature, 359(6398), 819-821.

Shuvalov, V., 2003, Displacement of target material during impact cratering, *in* Koeberl, C., Martinez-Ruiz, F. (eds.), Impact Markers in the Stratigraphic record, Impact Studies: Heidelberg, Springer, 121-135.

Stöffler, D., Artimieva, N.A., Ivanov, B.A., 2004, Origin and emplacement of the impact formations at Chicxulub, Mexico, as reveled by the ICDP deep drilling at Yaxcopoil-1 and by numerical modeling: Meteoritics and Planetary Science, 39(7), 1035-1067.

Sweetkind, D.S., Reynolds, R.L., Sawyer,, D.A., Rosenbaum, J.G., 2012 (1993), Effects of hydrothermal alteration on the magnetization of the Oligocene Carpenter Ridge Tuff, Bachelor Caldera, San Juan Mountains, Colorado: Journal of Geophysical research, v. 98, 6255-6266.

Sweetkind, D.S., Reynolds, R.L., Sawyer,, D.A., Rosenbaum, J.G., 1993, Effects of hydrothermal alteration on the magnetization of the Oligocene Carpenter Ridge Tuff, Bachelor Caldera, San Juan Mountains, Colorado: Journal of Geophysical research, 98(B4), 6255-6266.

Tarling, D.H., Hrouda, F., 1993, The Magnetic Anisotropy of Rocks: London, Chapman and Hall, 217 pp.

Tuchscherer, M.G., Reimold, W.U., Gibson, R.L., DeBruin, D., Spaeth, A., 2006, Major and trace element compositions of melt particles and associated phases from the Yaxcopoil-1 drill core, Chicxulub impact structure, Mexico: Meteoritics and Planetary Science, 41(9), 1361-1379.

Urrutia-Fucugauchi, J. Pérez-Cruz, L., 2008, Post-impact carbonate deposition in the Chicxulub impact crater region, Yucatán platform, Mexico: Current Science, 95(2), 241-252.

Urrutia-Fucugauchi, J., Pérez-Cruz, L., 2009, Multiring-forming large bolide impacts and evolution of planetary surfaces: International Geology Review, 51(12), 1079-1102. doi: 10.1080/002068 10902867161.

Urrutia-Fucugauchi, J., L. Marin, V.L. Sharpton, 1994, Reverse polarity magnetized melt rocks from the Cretaceous/Tertiary Chicxulub structure, Yucatán peninsula, Mexico: Tectonophysics, 237(1),105-112.

Urrutia-Fucugauchi, J., Marin, L., Trejo, A., 1996, UNAM scientific drilling program of Chicxulub impact structure: evidence of a 300 km crater diameter: Geophysical Research Letters, 23(13), 1565-1568.

Urrutia-Fucugauchi, J., Morgan, J.V., Stöffler, D., Claeys, P., 2004a, The Chicxulub Scientific Drilling Project (CSDP): Meteoritics and Planetary Science, 39(6), 787-790.

Urrutia-Fucugauchi, J., Soler, A.M., Rebolledo-Vieyra, M., Vera, P., 2004b, Paleomagnetic and rock magnetic study of the Yaxcopoil-1 impact breccia sequence, Chicxulub impact crater (Mexico): Meteoritics and Planetary Science, 39(6), 843-856.

Urrutia-Fucugauchi, J., Chávez-Aguirre, J.M., Pérez-Cruz, L., de la Rosa, J.L., 2008, Impact ejecta and carbonate sequence in the eastern sector of Chicxulub crater: Comptes Rendus Geosciences, 340, 801-810.

Urrutia-Fucugauchi, J., Camargo-Zanoguera, A., Pérez-Cruz, L., Pérez Cruz, G., 2011, The Chicxulub multi-ring impact crater, Yucatán carbonate platform, Gulf of Mexico: Geofisica Internacional, 50(1), 99-127.

Wittmann, A., Kenkemann, T., Hecht, L., Stöffler, D., 2007, Reconstruction of the Chicxulub ejecta plume from its deposits in drill core Yaxcopoil-1: Geological Society America Bulletin, 119(9-10), 1151-1167.